

**AER excision and bead implantation.** Fertilized chicken eggs (SPAFAS) were incubated at 39 °C for ~72–80 h. After staining with a dilute Nile Blue solution, the AER from the right forelimb was surgically excised and the embryo was incubated for the time specified and was then fixed in 4% paraformaldehyde. Heparin acrylic beads, of ~200 µm in diameter, were soaked in 1 mg ml<sup>-1</sup> FGF-4 (R&D Systems) for 1 h at ambient temperature. One bead was stapled onto the posterior mesenchyme of a stage-20 forelimb from which the AER was excised.

**Virus preparation and infections.** An EcoRI fragment of BS(Sk)-IκB-αΔN of 0.9 kb was subcloned into a ClaI2-Nco adaptor plasmid and then into RCAS-BP(A)<sup>27</sup>. RCAS viral stocks were produced as described<sup>28</sup>. The vector rAd-αΔN was constructed by ligating the 0.9-kb Acc651 fragment of pBS(SK)-IκB-αΔN into the Acc651 site of vector pAC. Identical construct formation was used for wild-type IκB-α, pAC-IκBα. We used a modified procedure from ref. 29 to prepare adenoviruses; additional details will be supplied upon request. Fertilized chicken eggs were incubated at 39 °C for 36–96 h. The eggs were windowed and the region to be infected stained with Nile Blue. Virus was loaded into a capillary pipet, attached to a picospritzer II and delivered at 10 p.s.i. in three pulses of 30 ms. For injections within the entire limb, virus was injected at 12–16 locations, depending on the limb size. For infection of a specific region, for example, the ZPA, eight injections were performed within that region. The egg was reintubated for 36 h or 7 days before being fixed in 4% paraformaldehyde for *in situ* hybridization or in 5% trichloroacetic acid (TCA) for cartilage staining, respectively.

**Cartilage staining.** TCA-fixed embryos were stained overnight in 0.075% Alcian Blue in acid alcohol, partially destained in 2% aqueous KOH, dehydrated in 100% ethanol and cleared in methyl salicylate.

**Scanning electron microscopy.** Samples were fixed in 3% glutaraldehyde buffered to pH 7.3 with sodium cacodylate. Following post-fixation in OsO<sub>4</sub>, they were dehydrated, critical-point dried, and sputter-coated with gold before viewing in a Hitachi S-500 scanning electron microscope.

Received 20 October 1997; accepted 2 February 1998.

- Nüsslein-Volhard, C., Lohs-Schardin, M., Sander, K. & Cremer, C. A dorso-ventral shift of embryonic primordia in a new maternal-effect mutant of *Drosophila*. *Nature* **283**, 474–476 (1980).
- Hamburger, V. & Hamilton, H. L. A series of normal stages in the development of the chick embryo. *J. Exp. Morphol.* **88**, 49–92 (1951).
- Summerbell, D. A quantitative analysis of the effect of the excision of the AER from the chick limb bud. *J. Embryol. Exp. Morphol.* **32**, 651–660 (1974).
- Fallon, J. F. et al. FGF-2: apical ectodermal ridge growth signal for chick limb bud development. *Science* **264**, 104–107 (1994).
- Niswander, L., Tickle, C., Vogel, A., Booth, I. & Martin, G. R. FGF-4 replaces the apical ectodermal ridge and directs outgrowth and patterning of the limb. *Cell* **75**, 579–587 (1993).
- Vogel, A., Rodriguez, C. & Izpisua-Belmonte, J. C. Involvement of FGF-8 in initiation, outgrowth and patterning of the vertebrate limb. *Development* **122**, 1737–1750 (1996).
- Crossley, P. H., Minowada, G., MacArthur, C. A. & Martin, G. R. Roles for FGF8 in the induction, initiation and maintenance of chick limb development. *Cell* **84**, 127–136 (1996).
- Inoue, J.-i. et al. Direct association of pp40/IκBβ with rel/NF-κB transcription factors: role of ankyrin repeats in the inhibition of DNA binding activity. *Proc. Natl Acad. Sci. USA* **89**, 4333–4337 (1992).
- Brockman, J. A. et al. Coupling of a signal response domain in IκBα to multiple pathways for NF-κB activation. *Mol. Cell. Biol.* **15**, 2809–2818 (1995).
- Treanckner, E. B.-M. et al. Phosphorylation of human IκB-α on serines 32 and 36 controls IκB-α proteolysis and NF-κB activation in response to diverse stimuli. *EMBO J.* **14**, 2876–2883 (1995).
- Grumont, R. J., Richardson, I. B., Gaff, C. & Beronidakis, S. Rel/NF-κB nuclear complexes that bind κB sites in the murine c-rel promoter are required for constitutive c-rel transcription in B cells. *Cell Growth Differ.* **4**, 731–743 (1993).
- Laufer, E., Nelson, C. E., Johnson, R. L., Morgan, B. A. & Tabin, C. Sonic hedgehog and FGF-4 act through a signaling cascade and feedback loop to integrate growth and patterning of the developing limb bud. *Cell* **79**, 993–1003 (1994).
- Niswander, L., Jeffrey, S., Martin, G. R. & Tickle, C. A positive feedback loop coordinates growth and patterning in the vertebrate limb. *Nature* **371**, 609–612 (1994).
- Jiang, J., Kosman, D., Ip, Y. T. & Levine, M. The dorsal morphogen gradient regulates the mesoderm determinant *twist* in early *Drosophila* embryos. *Genes Dev.* **5**, 1881–1891 (1991).
- Pan, D., Huang, J.-D. & Courey, A. J. Functional analysis of the *Drosophila twist* promoter reveals a dorsal-binding ventral activator region. *Genes Dev.* **5**, 1892–1901 (1991).
- Huang, J. D., Schwyter, D. H., Shirokawa, J. M. & Courey, A. J. The interplay between multiple enhancer and silencer elements defines the pattern of decapentaplegic expression. *Genes Dev.* **7**, 694–704 (1993).
- Schwyster, D. H., Huang, J. D., Dubnicoff, T. & Courey, A. J. The decapentaplegic promoter region plays an integral role in the spatial control of transcription. *Mol. Cell. Biol.* **15**, 3960–3968 (1995).
- Gitelman, I. Twist protein in mouse embryogenesis. *Dev. Biol.* **189**, 205–214 (1997).
- Winnier, G., Blessing, M., Labosky, P. A. & Hogan, B. L. Bone morphogenetic protein-4 is required for mesoderm formation and patterning in the mouse. *Genes Dev.* **9**, 2105–2116 (1995).
- Yokouchi, Y. et al. BMP-2/-4 mediate programmed cell death in chicken limb buds. *Development* **122**, 3725–3734 (1996).
- Duprez, D. et al. Overexpression of BMP-2 and BMP-4 alters the size and shape of developing skeletal elements in the chick limb. *Mech. Dev.* **57**, 145–157 (1996).
- Saunders, J. W., Jr & Gasseling, M. T. In *Epithelial-Mesenchymal Interaction* (eds Fleischmayer, R. & Billingham, R. E.) 78–97 (Williams and Wilkins, Boston, 1968).
- Ros, M., Lyons, G. & Fallon, J. Spatial and temporal analysis of homeobox genes expressed in chick limb buds by whole mount *in situ* hybridization. *Prog. Clin. Biol. Res.* **383A**, 79–87 (1993).

- Echelard, Y. et al. *Sonic hedgehog*, a member of a family of putative signalling molecules, is implicated in the regulation of CNS parity. *Cell* **75**, 1417–1430 (1993).
- Winnier, G. E., Hargett, L. & Hogan, B. L. The winged helix transcription factor MFH1 is required for proliferation and patterning of paraxial mesoderm in the mouse embryo. *Genes Dev.* **11**, 926–940 (1997).
- Wall, N. A. & Hogan, B. L. Expression of bone morphogenetic protein-4 (BMP-4), bone morphogenetic protein-7 (BMP-7), fibroblast growth factor-8 (FGF-8) and sonic hedgehog (SHH) during branchial arch development in the chick. *Mech. Dev.* **53**, 383–392 (1995).
- Hughes, S. H., Greenhouse, J. J., Petropoulos, C. J. & Suttrave, P. Adaptor plasmids simplify the insertion of foreign DNA into helper-independent retroviral vectors. *J. Virol.* **61**, 3004–3012 (1987).
- Morgan, B. A. & Fekete, D. M. Manipulating gene expression with replication-competent retroviruses. *Methods Cell Biol.* **51**, 185–218 (1996).
- Becker, T. C. et al. Use of recombinant adenovirus for metabolic engineering of mammalian cells. *Methods Cell Biol.* **43**, 161–176 (1994).

Supplementary information is available on Nature's World-Wide Web site (<http://www.nature.com>) or as paper copy from Mary Sheehan at the London editorial office of Nature.

**Acknowledgements.** We thank B. L. M. Hogan, J. Barnett, C. Wright, D. Bader, L. Rollins-Smith, and members of the Kerr laboratory for helpful discussions and critical review of this manuscript. A. McMahon for avian *Shh* cDNA; B. Hogan for the *M-Twist* and *Bmp-4* cDNA; C. B. Newgard for the adenoviral shuttle and wild-type vectors; S. Hughes for RCAS-BP(A) and RCAS-AlkPhos vectors; C. McCarther for the *Fgf-8* cDNA; C. Tabin for *cHoxA* and *cHoxD* cDNA series. This work was supported by a NIH grant, the American Cancer Society, and gene therapy pilot funds from the Vanderbilt Cancer Center Grant and MSKCC Support Grant. P.B.B. is a predoctoral fellow supported by a NIH training grant. L.D.K. is a recipient of an ACS Junior Faculty Research Award and a Cancer Research Institute Investigator Award.

Correspondence and requests for materials should be addressed to L.D.K. (e-mail: [KerrLD@ctr.vax.vanderbilt.edu](mailto:KerrLD@ctr.vax.vanderbilt.edu)).

## A proteolytic system that compensates for loss of proteasome function

Rickard Glas\*†, Matthew Bogoy\*†, John S. McMaster†, Maria Gaczynska† & Hidde L. Ploegh†

Center for Cancer Research, Department for Biology, Massachusetts Institute of Technology, 77 Massachusetts Avenue, Cambridge, Massachusetts 02139-4307, USA

\* These authors contributed equally to this work

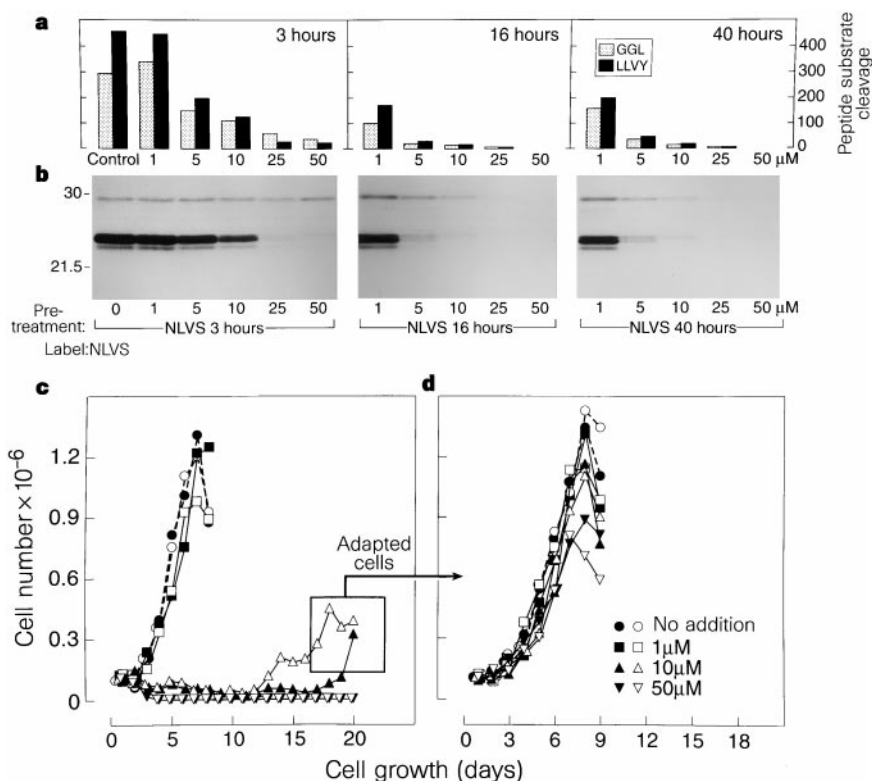
Proteolysis is essential for the execution of many cellular functions. These include removal of incorrectly folded or damaged proteins<sup>1</sup>, the activation of transcription factors<sup>2</sup>, the ordered degradation of proteins involved in cell cycle control<sup>3</sup>, and the generation of peptides destined for presentation by class I molecules of the major histocompatibility complex<sup>4</sup>. A multisubunit protease complex, the proteasome<sup>5</sup>, accomplishes these tasks. Here we show that in mammalian cells inactivation of the proteasome by covalent inhibitors allows the outgrowth of inhibitor-resistant cells. The growth of such adapted cells is apparently maintained by the induction of other proteolytic systems that compensate for the loss of proteasomal activity.

Proteasomal function can be inhibited pharmacologically by covalent or non-covalent modification of proteasomal β-subunits. Peptide aldehydes<sup>6</sup> act by forming a reversible hemiacetal adduct with Thr 1 on catalytically active β-subunits<sup>6,7</sup>, whereas the natural product lactacystin irreversibly alkylates Thr 1<sup>8–11</sup>. An amino-terminally modified tri-leucine vinyl sulphone, NIPL<sub>3</sub>-VS (NLVS), is a selective, covalent inhibitor that penetrates cell membranes and can be used to inhibit proteasomes in living cells<sup>12</sup>. NLVS and related peptide vinyl sulphones selectively and covalently modify all three catalytically active (X, Y and Z) β-subunits, as well as the γ-interferon-inducible β-subunits (LMP2, LMP7 and MECL-1), with little or no crossreaction with non-proteasomal proteases<sup>12</sup>.

EL-4 lymphoma cells, maintained in the presence of 10 µM NLVS, have drastically reduced proteasomal activity and die after 24–48 hours (Fig. 1). Homogenates from such EL-4 cells show

† Present addresses: Department of Pathology, Harvard Medical School, 200 Longwood Avenue, Boston, Massachusetts 02115, USA (R.G., M.B. and H.L.P.); University of Utah Department of Biochemistry, Salt Lake City, Utah 84132, USA (J.McM.); Department of Molecular Medicine, Institute of Biotechnology, University of Texas Health Science Center, San Antonio, Texas 78245, USA (M.G.).

**Figure 1** Covalent modification of proteasomes in EL-4 cells cultured in the presence of NLVS blocks enzymatic activity. The block in proteasomal activity inhibits cellular proliferation, but a minor population of EL-4 cells adapts to lethal concentrations of NLVS after prolonged culture. **a**, EL-4 cells were incubated in the presence of unlabelled NLVS for the indicated times and cellular homogenates of these cells were tested against the fluorogenic peptide substrates suc-LLVY-MCA (grey bars) and Z-GGL-MCA (black bars), showing progressive loss of enzymatic activity in a concentration- and time-dependent manner. **b**, Cellular homogenates in **a** were labelled with [<sup>125</sup>I]NLVS. **c**, EL-4 cells (100,000 cells per well) were cultured with the indicated concentrations of NLVS and counted daily. **d**, Cells recovered from 10 μM NLVS were adapted to grow in the presence of 50 μM NLVS by gradually increasing the concentration of NLVS during culture.



reduced hydrolysis of proteasome-preferred fluorogenic peptide substrates (Fig. 1a). Moreover, their proteasomal β-subunits are refractory to modification with <sup>125</sup>I-labelled NLVS (Fig. 1b). The lowest concentration of NLVS required to block proteasomal activity (5–10 μM) also inhibits the growth of EL-4 cells (Fig. 1a–c); the toxic and inhibitory effects of NLVS depend on its tri-leucine sequence, indicating that the toxicity is due to inhibition of the proteasome (data not shown). In contrast, prolonged exposure of EL-4 cells to the corresponding tri-leucine peptide aldehyde inhibitor (Z-L<sub>3</sub>-H) is toxic at 0.5–1.0 μM, a concentration at which there is only minimal inhibition of proteasomal proteolysis<sup>4,12</sup>.

Although most EL-4 cells cultured in the presence of 10 μM NLVS die (Fig. 1), after 2–3 weeks a minor population of EL-4 cells recovers and grows (termed adapted cells; Fig. 1c, d). Limiting dilution indicated a frequency of growth of ~1 in 300 cells in the presence of 10 μM NLVS, whereas 50 μM NLVS did not allow any recovery of cell growth (data not shown; Fig. 1c). This frequency of adaptation rules out mutation as the cause of resistance to NLVS, as does the observation that removal of NLVS allows recovery of proteasomal activity after 24 h of culture (data not shown). EL-4 cells, adapted to grow in up to 50 μM NLVS by gradually increasing the concentration of the inhibitor, had a growth rate similar to normal EL-4 cells. In overgrown cultures, adapted EL-4 cells died more rapidly than control cells, which could be due to effects on cellular metabolism by high concentrations of NLVS when nutrients are limiting (Fig. 1d).

Exposure of intact cells to [<sup>125</sup>I]NLVS showed labelling of control but not of adapted EL-4 cells, indicating prior modification of proteasomal β-subunits. To rule out the possibility that a change in membrane permeability of adapted cells prevents access of NLVS to the proteasome, proteolytic activity was monitored in cellular homogenates. Hydrolysis of proteasome substrates Z-GGL-MCA, Suc-LLVY-MCA (both substrates for the chymotrypsin-like activity) and Z-LLE-βNA (substrate for the PGPH (post glutamyl peptide hydrolysing activity) was reduced in adapted EL-4 cells to about 10–25% of control values, and labelling of proteasomal β-subunits by [<sup>125</sup>I]NLVS was largely absent (data not shown). Gel

filtration and the assay of individual fractions for hydrolysis of the Suc-LLVY-MCA substrate showed a characteristic pattern of 20S proteasome (Fig. 2a: main peak fractions, 20–25) and 26S proteasome (Fig. 2a: shoulder fractions 16–19) activities in EL-4 cells, whereas very little activity (<10%) remained in extracts prepared from adapted EL-4 cells (Fig. 2a). Upon addition of [<sup>125</sup>I]NLVS, we observed labelling of proteasomal β-subunits in fractions from control cells, corresponding to the peak of Suc-LLVY-MCA hydrolytic activity, but no labelling was detectable in fractions from adapted cells (Fig. 2b). These combined results indicate that the reduced proteasomal activity in adapted cells is attributable to covalent modification of β-subunits by NLVS.

We immunoprecipitated proteasomes from [<sup>35</sup>S]methionine-

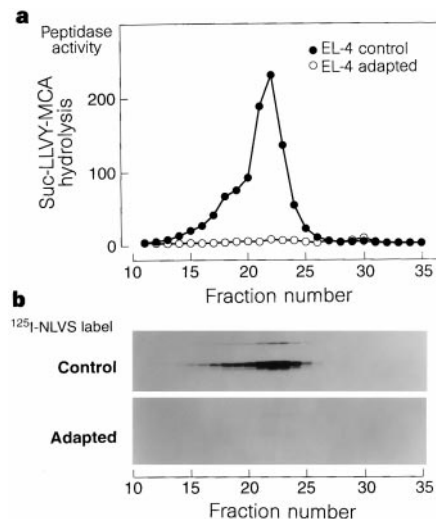


**Figure 2** Peptidase activity from EL-4-adapted and control fractions resolved by gel filtration (see Methods). Cytosolic fractions were centrifugated at high speed and the pellets were resuspended and fractionated on a Superose-6 column. Each fraction was tested for peptidase activity (**a**) and labelled with [<sup>125</sup>I]NLVS (**b**).

labelled control and adapted EL-4 cells with an antiserum against the proteasomal C9  $\alpha$ -subunit. Analysis by two-dimensional SDS-PAGE showed the characteristic pattern of  $\alpha$ - and  $\beta$ -subunits<sup>13</sup>. The relative intensities of the spots corresponding to  $\beta$ -subunits varied slightly, but the labelling pattern was comparable for EL-4 and adapted EL-4 cells (Fig 3a, b). The most obvious change was a comigration of LMP7 and LMP8 in proteasomes from adapted cells due to a shift in mobility of NLVS-modified LMP7 (Fig. 3b; indicated as LMP7\*). This was confirmed *in vitro* by showing that NLVS-treatment of isolated proteasomal subunits from EL-4 cells also resulted in comigration of NLVS-modified LMP7 with LMP8 (Fig. 3c, d).

Proteasomal proteolysis has been implicated in the generation of major histocompatibility complex (MHC) class I bound peptides<sup>4,14-17</sup>. Exposure of cells to either peptide aldehydes or lactacystin causes a temporary deficiency in the supply of peptides for MHC class I molecules<sup>4,16</sup>, leading to a reduction in the amount of assembled MHC class I products. In EL-4 cells, newly synthesized class I heavy chains rapidly form stable complexes with  $\beta_2$ -microglobulin ( $\beta_2$ m) and acquire complex-type glycans (Fig. 4a, d). In EL-4 cells treated with NLVS, there is a substantial reduction in the formation of assembled MHC class I complexes. As reported for L929 cells<sup>18</sup>, we do not observe complete inhibition of MHC class I assembly and transport, suggesting that non-proteasomal proteases may contribute a fraction of MHC class I-presented peptides in these cells (Fig. 4). Addition of MHC-binding peptide to cell lysates restored the recovery of assembled MHC class I molecules that lack terminal glycan modifications, which indicates an arrest of intracellular transport caused by a shortage of MHC ligands (Fig. 4b, e). However, NLVS-adapted EL-4 cells displayed almost normal levels of stable and therefore peptide-loaded MHC class I molecules which indicates that there is a non-proteasomal source of MHC ligands (Fig. 4).

In non-adapted EL-4 cells treated with the proteasome inhibitor NLVS, degradation of ubiquitinated proteins is inhibited, as shown by an increase in ubiquitin-conjugated material (relative molecular masses of 50K-200K) revealed by immunoblotting (data not shown). Staining the DNA of these cells with propidium iodide showed an increased fraction of cells in the G2/M (41% in G2) phase of the cell cycle in comparison with control cells (23% in G2),

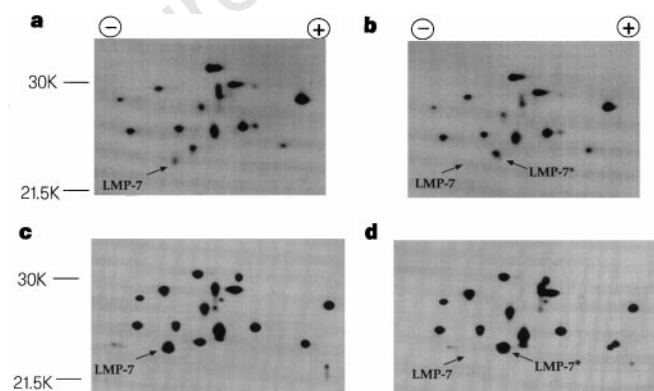


**Figure 3** Synthesis and assembly of proteasome subunits is normal in adapted cells. **a-d**, Adapted and control EL-4 cells were pulse-labelled for 1 h and chased for 24 h. Proteasomes were immunoprecipitated from either normal EL-4 cells (**a**) or adapted EL-4 cells (**b**) by using an anti-C9 ( $\alpha$ -subunit) polyclonal antiserum. **c, d**, EL-4 proteasomes were precipitated using a rabbit polyclonal antiserum raised against purified mouse proteasomes. These proteasomes were either not treated (**c**) or treated *in vitro* with 10  $\mu$ M unlabelled NLVS for 2 h (**d**). Samples were separated by two-dimensional non-equilibrium pH gradient electrophoresis and subunits visualized by fluorography. Note that the relative intensities of spots are the same for control and adapted cells, except for LMP-7 (NLVS-modified LMP7 comigrating with LMP8 is indicated as LMP7\*). The spot corresponding to LMP7 was identified by its relative molecular mass and isoelectric point<sup>13</sup>.

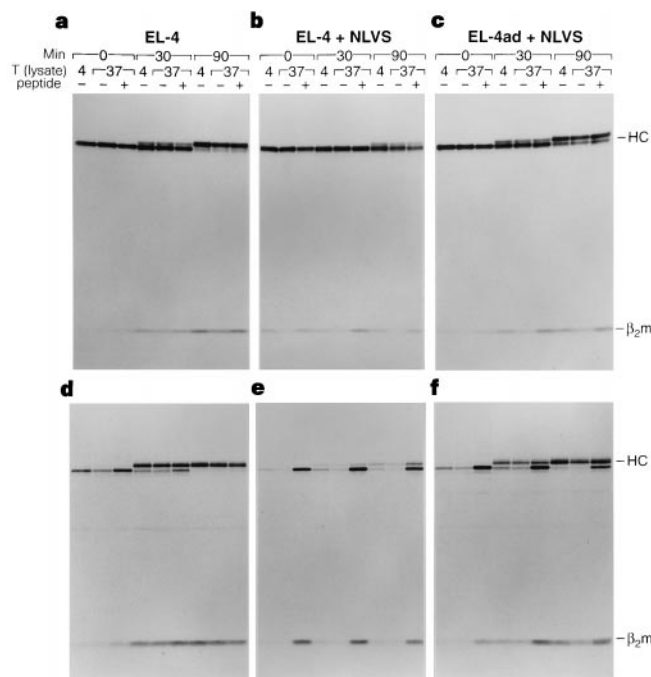


**Figure 4** Adapted EL-4 cells generate ligands for stable assembly and intracellular transport of MHC class I molecules. Cells were pulsed with [<sup>35</sup>S] methionine for 10 min and chased for the indicated times. The cells used were EL-4 (**a, d**), NLVS-treated EL-4 (**b, e**) and NLVS-adapted EL-4 (**c, f**). To assess total levels of class I heavy chain, regardless of peptide occupancy or state of assembly, we used an antiserum (anti-p8) against the cytoplasmic tail of H-2K<sup>b</sup> (**a-c**). To detect properly conformed H-2K<sup>b</sup> molecules, we used the monoclonal antibody Y3 (**d-f**). Lysates were exposed to 37°C for 20 min in the presence or absence of 10  $\mu$ M of an H-2K<sup>b</sup>-binding peptide (SIINFEKL), or were kept at 4°C. Only peptide-stabilized class I molecules maintain their conformation (Y3-reactive) at 37°C. Bands corresponding to the heavy chain (HC) and  $\beta_2$ -m are indicated.

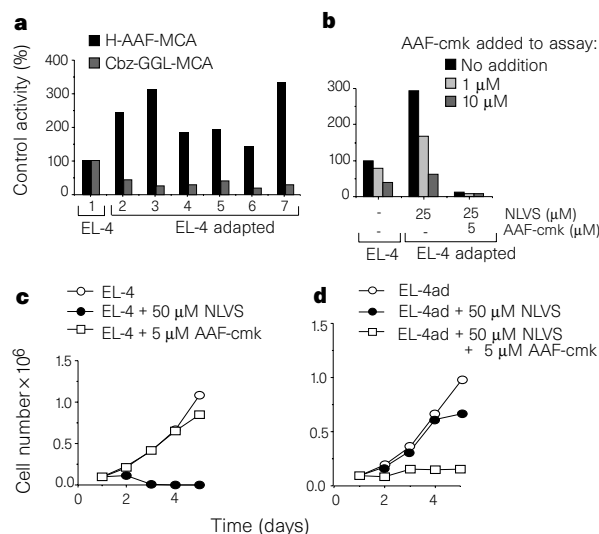


**Figure 5** AAF-MCA hydrolysis is increased in adapted cells. **a**, Cytosol prepared from independent cultures (bars 2-7) of adapted EL-4 cells shows increased hydrolysis of AAF-MCA peptide substrate and decreased hydrolysis of Cbz-GGL-MCA (proteasome substrate) compared with EL-4 (bar 1). **b**, The cytosolic activity that cleaves AAF-MCA is blocked by AAF-CMK both *in vivo* and *in vitro*. **c, d**, Inhibition of AAF cleavage is growth-inhibitory for adapted EL-4 cells (**d**) but not for control EL-4 cells (**c**).

consistent with proteasomal proteolysis being required at the G2/M–G1 transition<sup>3,19–21</sup>. In adapted EL-4 cells growing in the presence of NLVS, no cells accumulated in the G2/M phase (25% in G2), and the levels of ubiquitinated proteins were comparable to those in untreated EL-4 cells (data not shown). Thus, in adapted EL-4 cells, cell-cycle progression (Fig. 1d) and degradation of ubiquitinated proteins continue in the absence of normal proteasomal function.

The occurrence of a large ( $M_r > 1,000K$ ) protease complex in *Thermoplasma*, termed tricorn protease<sup>22</sup>, inspired us to examine the possibility of similar large complexes in adapted cells that could functionally replace proteasomal activity. Tricorn protease is resistant to proteasomal inhibitors and, characteristically, hydrolysis of the AAF-MCA substrate requires a free amino terminus. We indeed observed a remarkable increase in AAF-hydrolysing activity in adapted compared with normal EL-4 cells (Fig. 5a).

Although the active site of the tricorn protease has not yet been identified, it may contain a serine nucleophile<sup>22</sup>. As chloromethylketones are potent irreversible inhibitors of serine proteases<sup>23</sup>, we synthesized AAF-chloromethylketone (AAF-CMK) and found that it blocked AAF-hydrolysing activity in a dose-dependent manner, achieving >80% inhibition *in vitro* at 10  $\mu M$  AAF-CMK (Fig. 5b) without inhibiting proteasomal activity. If the AAF-MCA hydrolysing activity in adapted cells can compensate for loss of the proteasome, then inhibiting this activity should prevent growth of adapted EL-4 cells. There was no effect of 5  $\mu M$  AAF-CMK on the growth of normal EL-4 cells, whereas proliferation of adapted EL-4 cells was inhibited (Fig. 5c, d). The AAF-MCA cleaving activity must therefore be part of a protease or protease complex that contributes to or is required for survival of adapted cells.

To distinguish the induced protease activity, from the proteasome, we isolated material by centrifugation of cytosol for 5 hours at 100,000g, fractionated this by gel filtration, and tested each fraction for its capacity to hydrolyse AAF-MCA (Fig. 6; solid lines). The peak of AAF-MCA hydrolysing activity resolved from the void volume and eluted before the 20S and 26S proteasomes (Fig. 6). The AAF-hydrolytic activity is thus associated with a complex larger than the proteasome. This activity cannot be inhibited by NLVS, whereas addition of 10  $\mu M$  AAF-CMK blocks it completely (data not shown, and Fig. 5). Analysis by SDS-PAGE and silver staining showed that in control cells there was a cluster of proteasomal  $\beta$ -subunit-sized polypeptides of 20K–30K in fractions that cleave the proteasome substrate LLVY-MCA, and in adapted cells there was a complex set of polypeptides in the fractions that cleave AAF-MCA.

Proteasomal proteolysis can usually not be compromised without inhibiting proliferation<sup>5,24</sup> (Fig. 1). We have described the outgrowth of cells that, upon prolonged exposure to the proteasome inhibitor NLVS, appear to be resistant to the inclusion of otherwise toxic concentrations of this inhibitor. In these adapted cells there is

an increase in enzymatic activity capable of hydrolysing AAF-MCA which appears to be essential for the cells to grow when proteasomal activity is blocked. This activity is separable from both 26S and 20S proteasomes in specificity, size and inhibition profile. We propose that a minority of cells express auxiliary proteases. In the absence of proteasomal inhibition, these cells have no obvious growth advantage and are not represented in appreciable numbers. In the continuous presence of NLVS, however, the rare cells that express more AAF-hydrolysing activity are spared and recover to expand after two weeks of culture, relying at least partly on AAF-hydrolysing activity to do so.

We conclude that proteasomes can be replaced functionally by other protease activities, which raises questions about the fate of ubiquitin-conjugated proteins in adapted cells, on the mechanisms used by adapted cells to regulate their cell cycle, and on the possible involvement of non-proteasomal cytosolic proteases in MHC class I-restricted antigen presentation. Destruction of cyclins and cyclin-dependent-kinase inhibitors has almost invariably been attributed to the ubiquitin-proteasomal system<sup>3,25–27</sup>. The detailed molecular characterization of the activities that allow adapted cells to survive will be a challenge. □

**Methods**

**Cells and cell culture.** The mouse lymphoma cell line EL-4 was maintained in Dulbecco's modified Eagle's or RPMI 1640 medium supplemented with 10% (v/v) fetal calf serum. Adapted EL-4 cells were maintained in the presence of 50  $\mu M$  5-iodo-4-hydroxy-nitrophenyl acetyl-leucyl-leucyl-leucine vinyl sulphone<sup>12</sup>.

**Inhibitors.** [<sup>125</sup>I]NIP-L<sub>3</sub>-VS and NIP-L<sub>3</sub>-VS (NLVS) were synthesized as described<sup>12</sup>. All inhibitors were added to lysates and to cells by dilution of a dimethylsulphoxide (DMSO) stock solution such that the final concentration of DMSO was 1%.

**Antibodies.** Anti-C9 is a monoclonal antibody against a proteasomal  $\alpha$ -subunit in assembled proteasomes; rabbit anti-mouse proteasome is an antiserum directed against assembled mouse proteasomes (gift from J. Monaco)<sup>13</sup>; Y3 (ref. 28) is a monoclonal antibody that recognizes the  $\alpha 1/\alpha 2$  domain of properly folded mouse class I heavy chains; anti-P8 is a rabbit antiserum specific for exon 8 in the cytoplasmic tail of H-2K<sup>b</sup> mouse MHC class I heavy chains; and anti-ubiquitin is a polyclonal antiserum reactive against ubiquitin and ubiquitin conjugates (gift from A. L. Haas).

**Growth curves.** Cells (100,000 in 1 ml medium) were grown in the presence of inhibitor or DMSO (1%) in 24-well plates. Cells were resuspended daily, 20- $\mu l$  aliquots were removed and mixed with trypan blue dye (0.1%). Cells that excluded the dye were considered viable and were counted.

**Labelling of proteasomes with [<sup>125</sup>I]NIP-L<sub>3</sub>-VS.** Cells ( $1.5 \times 10^6$ ) or lysates (50  $\mu g$  unless otherwise indicated) were labelled with [<sup>125</sup>I]NLVS, diluted to a final concentration of  $1.8 \times 10^4$  Bq ml<sup>-1</sup> in tissue culture medium (cells) or buffer I (lysates; 50 mM Tris, pH 7.4, 2 mM DTT, 5 mM MgCl<sub>2</sub>, 2 mM ATP). Samples were incubated at 37 °C for 2 h then 1 $\times$  (cells) or 4 $\times$  (lysates) SDS-sample buffer was added. Proteins were separated by SDS-PAGE.

**Preparation of lysates from control EL-4, NLVS-treated or adapted cells.** Cells were washed in cold PBS, then in buffer I, and pelleted. Glass beads (<106 microns, acid-washed; Sigma) equivalent to the volume of the cellular pellet were added, followed by the same volume of homogenization buffer (50 mM Tris, pH 7.4, 1 mM DTT, 5 mM MgCl<sub>2</sub>, 2 mM ATP, 250 mM sucrose). Cells were vortexed for 1 min. Beads and cell debris were removed by centrifugation at 1,000g for 5 min, followed by 10,000g for 20 min. Protein concentration was determined using the BCA protocol (Pierce Chemical).

**Fluorogenic peptide substrate assay.** Peptidase activity was measured using the following fluorescent labelled peptide substrates: Suc-LLVY-MCA, Z-LLG-MCA and Suc-AAF-MCA for analysis of chymotrypsin-like activity of the proteasome; Boc-LRR-MCA for analysis of the trypsin-like activity of the proteasome; Z-LLE- $\beta$ -BNA for analysis of the PGPH activity of the proteasome; and AAF-MCA for analysis of non-proteasomal proteolysis. Partially purified proteasomes from 5-h pellets (5  $\mu g$  total protein), or total lysates (10  $\mu g$ ) were diluted to 100  $\mu l$  in only buffer I or 50 mM Tris, pH 7.4. Inhibitors and substrates (100  $\mu M$ ) were added to samples as DMSO stocks. Samples were

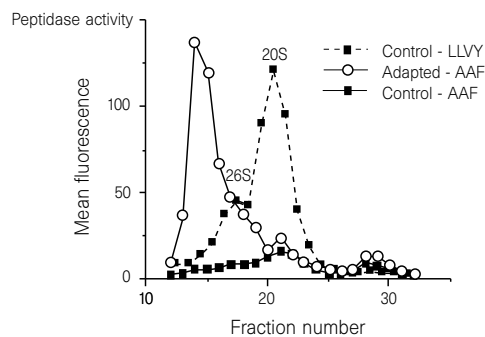


**Figure 6** AAF-MCA hydrolysing activity elutes before the proteasome, indicating that it has a higher  $M_r$ . Protein fractions from differential centrifugation of cytosols (see Methods) were fractionated on a Superose-6 gel filtration column as for Fig. 2. Fractions were assayed for hydrolysis of the non-proteasomal substrate AAF-MCA (solid lines) or Suc-LLVY-MCA (dashed line, indicating the elution of proteasomal activity).

incubated at 37°C for 45 min and the reaction was quenched with 1 ml 1% SDS. Fluorescence was measured using a Hitachi F4500 spectrofluorimeter.

**Class I assembly.** To monitor class I assembly, a pulse-chase experiment was done using EL-4 cells, EL-4 cells treated with 50 μM NLVS, or adapted EL-4 cells. NLVS-treated cells were pretreated with 50 μM NLVS for 16 h before the pulse chase<sup>4</sup>. Stabilization was assayed as described<sup>29</sup>, using the OVA peptide SIINFEKL. Class I molecules were isolated by immunoprecipitation using the Y3 monoclonal antibody or p8 antiserum. Proteins were separated by SDS-PAGE and visualized by fluorography.

**Gel filtration of subcellular fractions.** Lysates were prepared from control EL-4 and EL-4 adapted cells (2–3 × 10<sup>8</sup> cells) and fractionated by differential centrifugation. The 5-h 100,000g pellets were resuspended in 0.5 ml homogenization buffer (50 mM Tris, pH 7.0, 20% glycerol) and injected into a Superose-6 column (1.5 cm × 30 cm) at room temperature. The sample was eluted at a flow rate of 0.2 ml min<sup>-1</sup>. Fractions of 0.5 ml were collected and placed on ice. Aliquots of each fraction (20 μl) were used to measure hydrolysis of Suc-LLV-MCA and AAF-MCA.

Received 22 September 1997; accepted 2 January 1998.

1. Etlinger, J. D. & Goldberg, A. L. A soluble ATP-dependent proteolytic system responsible for the degradation of abnormal proteins in reticulocytes. *Proc. Natl Acad. Sci. USA* **74**, 54–58 (1977).
2. Palombella, V. J., Rando, O. J., Goldberg, A. L. & Maniatis, T. The ubiquitin-proteasome pathway is required for processing the NF-κB1 precursor protein and the activation of NF-κB. *Cell* **78**, 773–785 (1994).
3. Glotzer, M., Murray, A. W. & Kirschner, M. W. Cyclin is degraded by the ubiquitin pathway. *Nature* **349**, 132–138 (1991).
4. Rock, K. L. et al. Inhibition of the proteasome block the degradation of most cell proteins and the generation of peptides presented on MHC class I molecules. *Cell* **78**, 761–771 (1994).
5. Coux, O., Tanaka, K. & Goldberg, A. Structure and functions of the 20S and 26S proteasomes. *Annu. Rev. Biochem.* **65**, 801–847 (1996).
6. Seemuller, E. et al. The proteasome from *Thermoplasma acidophilum*: A threonine protease. *Science* **268**, 579–582 (1995).
7. Löwe, J. et al. Crystal structure of the 20S proteasome from the Archaeon *T. acidophilum* at 3.4 Å resolution. *Science* **268**, 533–539 (1995).
8. Omura, S. et al. Lactacystin, a novel microbial metabolite, induces neurogenesis of neuroblastoma cells. *J. Antibiot.* **44**, 113–116 (1991).
9. Fenteany, G. et al. Inhibition of proteasome activities and subunit-specific amino-terminal threonine modification by lactacystin. *Science* **268**, 726–730 (1995).
10. Dick, L. R. et al. Mechanistic studies on the inactivation of the proteasome by lactacystin. *J. Biol. Chem.* **271**, 7273–7276 (1996).
11. Groll, M. et al. Structure of 20S proteasome from yeast at 2.4 Å resolution. *Nature* **386**, 463–471 (1997).
12. Bogoy, M. et al. Covalent modification of the active site Thr of proteasomal β-subunits and the *E. coli* homolog HslV by a new class of inhibitors. *Proc. Natl Acad. Sci. USA* **94**, 6629–6634 (1997).
13. Nandi, D., Woodward, E., Ginsburg, D. B. & Monaco, J. J. Intermediates in the formation of mouse 20S proteasomes: implications for the assembly of precursor beta subunits. *EMBO J.* **16**, 5363–5375 (1997).
14. Driscoll, J., Brown, M. G., Finley, D. & Monaco, J. J. MHC-linked LMP gene products specifically alter peptidase activities of the proteasome. *Nature* **365**, 262–264 (1993).
15. Gaczynska, M., Rock, K. L. & Goldberg, A. γ-Interferon and expression of MHC genes regulate peptide hydrolysis by proteasomes. *Nature* **365**, 264–267 (1993).
16. Craiu, A. C. et al. Lactacystin and clasto-lactacystin β-lactone modify multiple proteasome β subunits and inhibit intracellular protein degradation and MHC class I antigen presentation. *J. Biol. Chem.* **272**, 13437–13445 (1997).
17. Bai, A. & Forman, J. The effect of proteasome inhibitor lactacystin on the presentation of transporter associated with antigen processing (TAP)-dependent and TAP-independent peptide epitopes by class I molecules. *J. Immunol.* **159**, 2139–2146 (1997).
18. Vinitzky, A. et al. The generation of MHC class I-associated peptides is only partially inhibited by proteasome inhibitors: involvement of non-proteasomal cytosolic proteases in antigen processing? *J. Immunol.* **159**, 554–564 (1997).
19. Hilt, W. & Wolf, D. H. Proteasomes of the yeast *S. cerevisiae*: genes, structure and function. *Mol. Biol. Rep.* **21**, 3–10 (1995).
20. Ghislain, M., Udvardy, A. & Mann, C. et al. *S. cerevisiae* 26S protease mutants arrest cell division in G2/metaphase. *Nature* **366**, 358–362 (1993).
21. Gordon, C., McGurk, G., Dillon, P., Rosen, C. & Hastie, N. D. Defective mitosis due to a mutation in the gene for a fission yeast 26S protease subunit. *Nature* **366**, 355–357 (1993).
22. Tamura, T. et al. Tricorn protease—the core of a modular proteolytic system. *Science* **274**, 1385–1389 (1996).
23. Kettner, C. & Shaw, E. Inactivation of trypsin-like enzymes with peptides of arginine chloromethyl ketone. *Meth. Enzymol.* **80**, 826–842 (1981).
24. Drexler, H. C. A. Activation of the cell death program by inhibition of proteasome function. *Proc. Natl Acad. Sci. USA* **94**, 855–860 (1997).
25. Hershko, A. & Ciechanover, A. The ubiquitin system for protein degradation. *Annu. Rev. Biochem.* **61**, 761–807 (1992).
26. King, R. W., Jackson, P. K. & Kirschner, M. W. Mitosis in transition. *Cell* **79**, 563–571 (1994).
27. Sheaff, R. & Roberts, J. M. End of the line: proteolytic degradation of cyclin-dependent kinase inhibitors. *Chem. Biol.* **3**, 869–873 (1996).
28. Hammerling, G. J., Rusch, E., Tada, N., Kimura, S. & Hammerling, U. Localization of allo-determinants on H-2<sup>D</sup> determined with monoclonal antibodies and H-2 mutant mice. *Proc. Natl Acad. Sci. USA* **79**, 4737–4741 (1982).
29. Ljunggren, H.-G. et al. Empty MHC class I molecules come out in the cold. *Nature* **346**, 476–480 (1990).

**Acknowledgements.** This work was supported by grants from the NIH and Boehringer Ingelheim. R. G. is a fellow of the The Swedish Foundation for International Cooperation in Research and High Education (STINT) Stockholm.

Correspondence and requests for materials should be addressed to H.L.P. (e-mail: ploegh@hms.harvard.edu).

## Rap1 mediates sustained MAP kinase activation induced by nerve growth factor

Randall D. York, Hong Yao, Tara Dillon, Cindy L. Ellig, Stephani P. Eckert, Edwin W. McCleskey & Philip J. S. Stork\*

The Vollum Institute for Advanced Biomedical Research, \* Department of Pathology, Oregon Health Sciences University, Portland, Oregon 97201, USA

Activation of mitogen-activated protein (MAP) kinase (also known as extracellular-signal-regulated kinase, or ERK)<sup>1</sup> by growth factors can trigger either cell growth or differentiation. The intracellular signals that couple growth factors to MAP kinase may determine the different effects of growth factors: for example, transient activation of MAP kinase by epidermal growth factor stimulates proliferation of PC12 cells<sup>1</sup>, whereas they differentiate in response to nerve growth factor, which acts partly by inducing a sustained activation of MAP kinase<sup>1</sup>. Here we show that activation of MAP kinase by nerve growth factor involves two distinct pathways: the initial activation of MAP kinase requires the small G protein Ras, but its activation is sustained by the small G protein Rap1. Rap1 is activated by CRK adaptor proteins and the guanine-nucleotide-exchange factor C3G, and forms a stable complex with B-Raf, an activator of MAP kinase. Rap1 is required for at least two indices of neuronal differentiation by nerve growth factor: electrical excitability and the induction of neuron-specific genes. We propose that the activation of Rap1 by C3G represents a common mechanism to induce sustained activation of the MAP kinase cascade in cells that express B-Raf.

PC12 cells are a well studied model of growth-factor specificity. Treatment of PC12 cells with nerve growth factor (NGF) triggers differentiation into sympathetic-like neurons, characterized by electrical excitability, the induction of a set of neuron-specific genes, and neurite outgrowth<sup>2,3</sup>. The ability of NGF to induce sustained activation of the ERK family of MAP kinases has been implicated in PC12 cell differentiation<sup>1,4–7</sup>. The molecular mechanisms responsible for sustaining ERK activation are not known. However, signals that limit ERK activation have been identified. In some cells, ERK directs the phosphorylation of the Ras guanine-nucleotide-exchange factor, Sos, to terminate Ras-dependent ERK activation<sup>8</sup>. Therefore, Ras-independent pathways may be required to maintain ERK activation for sustained periods. As Rap1 can also stimulate ERK in PC12 cells<sup>9</sup>, we examined whether Rap1 contributes to NGF action in PC12 cells.

Using an interfering mutant of Rap1, RapN17 (ref. 9), we showed that Rap1 is required for maximal activation of ERK by NGF in PC12 cells. RapN17 blocked the ability of NGF to stimulate the sustained phase of ERK activation in these cells, without inhibiting the initial rapid phase of ERK activation. In contrast, RasN17, a dominant-negative mutant of Ras, blocked only the initial phase of ERK activation by NGF (Fig. 1a). It has been suggested that Ras is essential for NGF signalling to ERKs<sup>10,11</sup>, but these studies investigated only early time points of stimulation by NGF or used stably transfected clonal variants of PC12 cells rather than wild-type cells. Our results indicate that Ras and Rap1 mediate the initial and the sustained phases of NGF-induced activation of ERK, respectively, and that Ras and Rap1 act largely independently of each other.

As one of the nuclear targets of ERK is Elk-1, a transcription factor of the Ets family<sup>9</sup>, NGF-induced activation of ERK can be monitored by measuring the rate of Elk-1-dependent transcription<sup>9</sup>. In PC12 cells, NGF stimulated Elk-1 more than did EGF (Fig. 1b). Expression of RapN17 reduced NGF-induced activation of Elk-1 to levels observed following stimulation by epidermal